Laser drilling of high aspect ratio holes in copper with femtosecond, picosecond and nanosecond pulses

A. Weck, T.H.R. Crawford, D.S. Wilkinson, H.K. Haugen, J.S. Preston

May 13, 2008

A. Weck
McMaster University, Department of Materials Science and Engineering. 1280 Main Street West, Hamilton, ON, Canada. weckag@mcmaster.ca

T.H.R. Crawford
Department of Engineering Physics, McMaster University, Hamilton, Ontario, Canada, L8S 4L7.

D. Wilkinson
McMaster University, Department of Materials Science and Engineering. 1280 Main Street West, Hamilton, ON, Canada.

H.K. Haugen
Department of Engineering Physics, McMaster University, Hamilton, Ontario, Canada, L8S 4L7.

J.S. Preston
Department of Engineering Physics, McMaster University, Hamilton, Ontario, Canada, L8S 4L7, also with the Department of Physics and Astronomy, McMaster University.

Abstract

Deep laser holes were drilled in copper sheets using various pulse lengths and environments. By recording the intensity on a photodiode placed under the sample while drilling the holes, the number of pulses to drill through the sheet was obtained as a function of pulse length and energy. The entrance diameter of the holes was successfully predicted using a Gaussian approximation and a material removal fluence threshold of 0.39 J/cm^2 for a pulse length of 150 fs. From cross sections of the holes, the morphology of the inside walls was observed and shows an increase in the amount of molten material with pulse length. A transition pulse length is defined as the point at which the laser affected material goes from being mainly vaporized to mainly melted. This transition occurs near $\sim$10 ps which corresponds approximately to the electron-phonon relaxation time for copper.
PACS 62.20.Mk;62.25.+g;79.20.Ds

1 Introduction

Although a significant amount of work has been done on laser-induced surface damage resulting in the formation of shallow holes [1, 2, 3, 4, 5], the production of high aspect ratio holes is also scientifically and technologically relevant (see, e.g., [1, 6, 7, 8, 9, 10]). Previous work on high aspect ratio holes has shown that ablated material is redeposited on the side of the holes [9]. Liquid ejection and nanoparticle formation can also occur and have an important impact on laser drilling [10, 11, 12]. It has been shown that lower pulse lengths lead to cleaner holes [1] and that at high fluences drilling rate is higher when the holes are drilled in vacuum versus air [13]. However, systematic quantitative studies are lacking on the effect of parameters such as pulse length and environment on the morphologies obtained inside the laser drilled hole.

Here we present a detailed study of high aspect ratio holes drilled in copper sheets. For the first part of this paper, the hole formation was monitored in-situ with a photodiode placed under the sample and we systematically varied the pulse energy and number of pulses per hole. Then the effect of pulse lengths, from 150 fs to 7 ns, on the entrance and inside hole morphology and on the photodiode signal was investigated. Finally, the differences between drilling in air versus vacuum are presented.

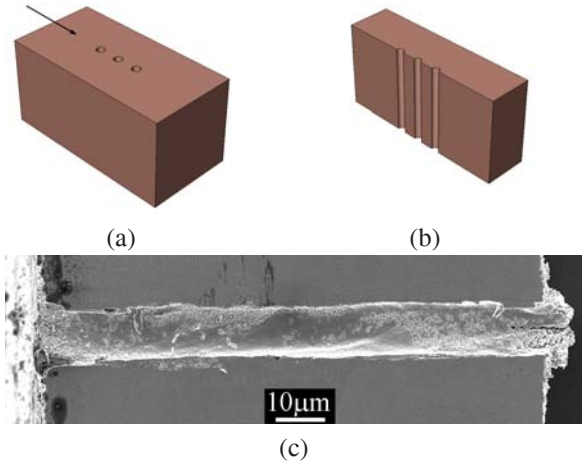

Figure 1: Schematic drawing showing (a) a 100 μm thick sheet containing 10 μm diameter through holes and (b) the results of a microtome cut. (c) Cross section of a laser hole drilled in air with 30000 pulses per holes and with a pulse length of 35 ps.

2 Experimental procedure

The material used is high purity copper (99.999%). It was received in the form of a 100 μm thick sheet and was annealed in order to achieve a grain size of the order of 300 μm. As the final laser holes are $\sim$10 μm in diameter, the laser holes drilled though the thickness of the sheet are drilled almost in a single crystal and we can neglect grain boundary effects. The laser set-up, which includes a vacuum chamber placed on a translation stage, is described elsewhere ([14]). Several parameters were varied, namely environment (air, and rough vacuum of $\sim$0.1 mbar), number of pulses per hole (from 1 to 30000 pulses) and incident pulse energy (from 0.89 to 20 μJ). Pulse energies were measured using a semiconductor power-meter with a quoted accuracy of $\pm$5%. For all experiments presented here, we used a rotating polarization obtained with a spinning zero order half wave plate (rotating $\sim$15°/ms). The same focusing element (5$\times$ microscope objective) was used in all cases providing a $\sim$5 μm spot radius. Pulses at 1 kHz repetition rate were obtained from a regeneratively amplified Ti:Sapphire laser system employing chirped pulse amplification. Pulse lengths (full-width half-maximum, FWHM) of approximately 150 fs, 300 fs, 600 fs, 1 ps, 3 ps, 10 ps and 35 ps were obtained by varying the pulse compression in the compression stage. A pulse length of $\sim$220 ps was obtained when by-passing the compressor stage and one of $\sim$7 ns by blocking the entry of seeded pulses into the amplifier. A non-collinear second-order autocorrelator with a 500 μm thick KDP crystal was used to determine pulse lengths except for the 7 ns case. In the latter case, a communications signal analyzer and an InGaAs photodiode with a manufacturer-quoted 18.5 ps FWHM impulse response were used.

In order to quantify the laser drilling process, a reverse-biased Si photodiode with an area of $\sim$1 cm^2 was placed under the sample. This photodiode was connected to a boxcar integrator which outputs to a data acquisition computer. As long as the laser hole does not reach the bottom of the sheet, the intensity on the photodiode is zero. An intensity increase from zero on the photodiode corresponds exactly to the point at which the laser just reached the bottom of the sheet. Furthermore, by recording the photodiode signal as the hole is being drilled, information on the hole broadening on the exit side and on the drilling process can also be obtained.

Finally, in order to obtain information on the morphology inside the hole, the laser holes were cut as shown in figure 1 using a microtome which consists of an extremely sharp diamond knife. This ensures a clean cut without introducing damage in the material. The cut was done without lubricant in order to preserve the interior of the hole as-drilled. The hole cross section was then observed in a scanning electron microscope as shown in figure 1(c).

3 Pulse energy and number of pulses per hole

3.1 Photodiode results

The parameters investigated in this section are the energy per pulse and the number of pulses per hole to drill through a 100 μm thick copper sheet. A pulse length of 150 fs and a spinning polarization were used while the drilling was done in air. Holes were drilled using several energies and 30000 pulses per hole. The signal from the photodiode placed under the sample is presented in figure 2 where arrows are relating the incoming laser pulse energy to the corresponding curves. A similar labelling

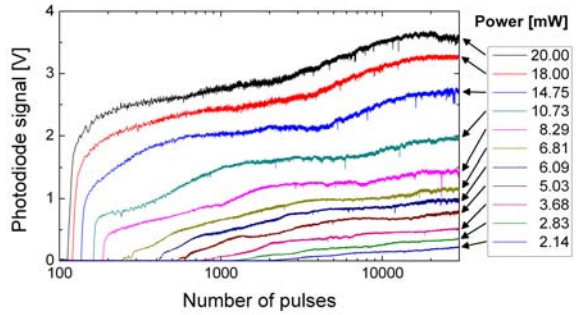

Figure 2: Results from the photodiode under the sample while drilling holes at 150 fs in air with various pulse energies.

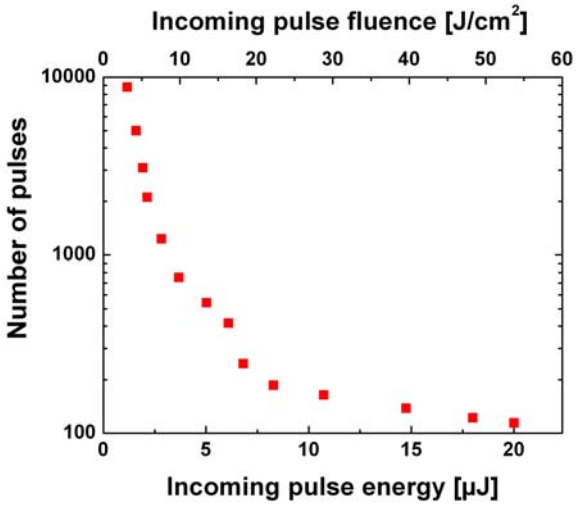

Figure 3: Number of pulses to go through the 100 μm thick copper sheet at 150 fs in air.

scheme is used for the other graphs in this paper, whereby decreasing pulse energies correspond to decreasing final intensities on the photodiode. In figure 2(b) the first deviation from zero photodiode signal corresponds to the point at which the laser just drilled through the sample. One can see that the higher the pulse energy, the lower the number of pulses required to drill through the sheet. The number of pulses to breakthrough as a function of the incoming energy can be extracted from figure 2(b) and is shown in figure 3. The increase in intensity after breakthrough is related to the increasing diameter of the exit hole. A steady state can be defined as the number of pulses at which the intensity on the photodiode does not vary significantly with number of pulses.

3.2 Entrance and exit hole diameters

The entrance and exit hole diameters were measured under an optical microscope after drilling with 30000 pulses, reaching an approximately steady state configuration. The evolution of the diameters as a function of incoming laser energy is shown in figure 4. It can be seen that the higher the energy, the larger the hole diameter and that the entrance hole diameters are larger than the exit hole diameters at a given energy. The higher the energy, the smaller the difference between the entrance and exit hole diameters. In the following, we attempt to predict the entrance hole diameters using a simple Gaussian approximation. Assuming that the laser beam has a Gaussian intensity profile, it is possible to calculate the fluence in the wings of the Gaussian using the general equation for the fluence of a Gaussian beam:

$$\phi(r) = \phi_\circ \exp\left(\frac{-2r^2}{\omega_\circ^2}\right) \qquad (1)$$

where $\phi(r)$ is the fluence at a distance r from the Gaussian middle axis and $\phi_\circ$ the fluence on the middle axis. This peak fluence is calculated from the incoming pulse energy E by $\phi_\circ = 2E/\pi\omega_\circ^2$. The parameter $\omega_\circ$ is defined as the radius at which the intensity has decreased to $1/e^2$ of its middle axis value. For the focusing objective used here, $\omega_\circ \approx 5$ μm.

In order to predict the steady state entrance hole diameters, a threshold fluence $\phi_{\rm th}$ is defined as the fluence below which material removal does not occur. In the early stages of drilling, when $\phi(r) \geq \phi_{\rm th}$ on the rim of the hole, the hole diameter is expected to increase until $\phi(r) < \phi_{\rm th}$. Therefore, the predicted steady state entrance radii $r_{\rm in}$ of the holes are defined for $\phi(r_{\rm in}) = \phi_{\rm th}$ as:

$$r_{\rm in} = \sqrt{\frac{\omega_\circ^2}{2} \ln\left(\frac{\phi_\circ}{\phi_{\rm th}}\right)}. \qquad (2)$$

A value of $\phi_{\rm th} \approx 0.39$ J/cm^2 was found to best fit the experimental results and the evolution of $r_{\rm in}$ with incoming laser energy is plotted in figure 4. Although the fit is

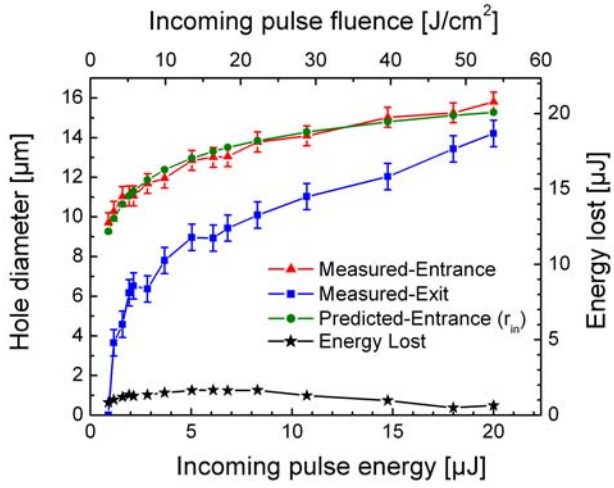

Figure 4: Experimentally measured entrance and exit hole diameters for laser holes drilled with 150 fs, 30000 pulses, in air for various energies. The predicted entrance hole diameter assumes a Gaussian beam profile with an ablation threshold $\phi_{\rm th}$=0.39 J/cm^2. The uncertainty on the experimental hole diameters measurement is $\pm$0.5 μm. Also shown is the pulse energy lost by the laser pulses passing through the hole after 30000 pulses as a function of incoming pulse energy.

restricted to data corresponding to the wings of the beam spatial profile, one can see that the prediction using a simple Gaussian approximation is in good agreement with the experimental results. The value of $\phi_{\rm th}$ $\approx$0.39 J/cm^2 is however somewhat larger than the values found in the literature for the fluence threshold of copper for comparable multiple pulse irradiation conditions [2, 15, 16] in the low-fluence ablation regime. The prediction of the exit hole diameter has not been attempted here due to the complexity of laser beam propagation within the hole which is difficult to precisely quantify.

The maximum photodiode signal at a given energy in figure 2(a) can be compared to the signal obtained using the same pulse energy but without the copper sheet present. The difference between these two voltages at steady state can be converted into absolute value of energy lost in the hole which is around 1 μJ (figure 4). Interestingly, this value is fairly independent of the energy of the laser beam.

4 Pulse length

4.1 Expected effects of pulse length

During laser micromachining of metals, the laser beam transfers first almost exclusively its energy to the conduction band electrons. Because the electron-electron energy transfer occurs over very short times, it is the electron-phonon relaxation time that controls material vaporization and/or melting when drilling with ultrashort laser pulses. For copper, the electron-phonon relaxation time is of the order of a few picoseconds [17, 18]. In the two-temperature model used to describe short pulse laser irradiation of metals, the nature of the material evolution process is affected by the laser pulse length with shorter pulses producing less molten material [1]. We expect a transition in the material removal mechanism and drilling efficiency for pulse lengths close to the electron-phonon relaxation time. However, this transition could be affected by various mechanisms such as plasma formation, material redeposition in the hole, and ejected material which could interfere with the incoming laser pulse. In the following sections, we investigate the effect of pulse length on hole morphology and photodiode signal.

4.2 Photodiode signal

The results obtained from the photodiode placed under the sample during the laser drilling process are presented in figure 5 and give more insight into the mechanisms of laser micromachining with ultrashort pulses. Up to a pulse length of 1 ps, the curves are very similar. However, for pulse lengths of 10 ps and 35 ps, the curves are much noisier, while for the 220 ps and 7 ns cases, the curves are less noisy again. This behavior might be attributed to plasma formation. Plasma effects associated with ultrashort pulse irradiation of solids are well known (see, e.g., [6, 19]). Mao et al. [20, 21] have discussed early-stage plasma effects associated with picosecond laser irradiation of a copper target, and concluded that laser-target-air interactions can be important for plasma initiation. The fluctuations in photodiode signal observed in the present work are most evident for pulses of intermediate duration, and under conditions where the hole size is not changing significantly. Further investigation will be required to elucidate the mechanisms.

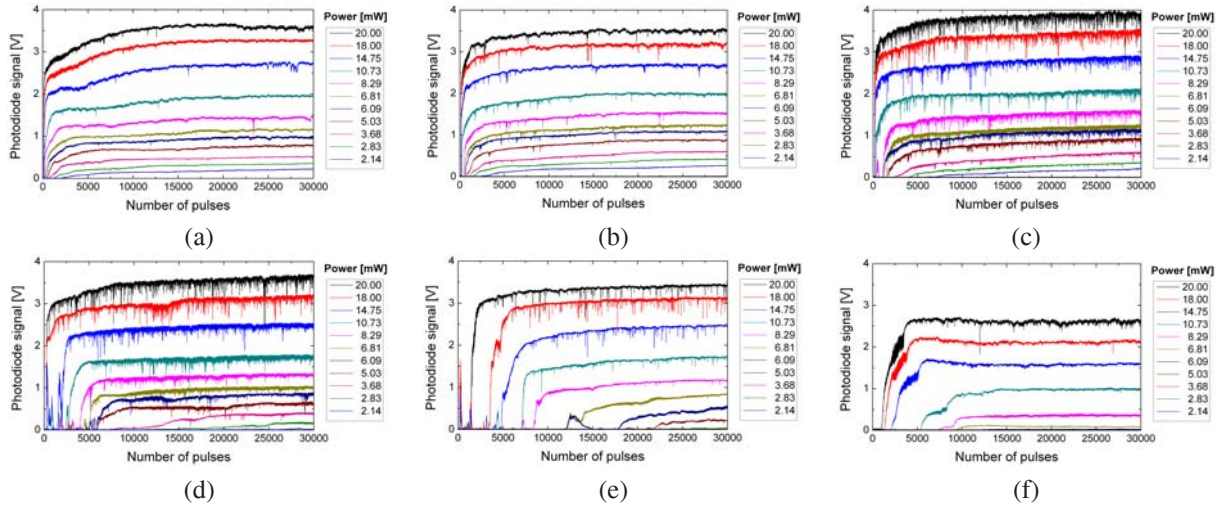

Figure 5: Photodiode results for holes drilled in air using 30000 pulses per hole. The pulse lengths presented here are (a) 150 fs, (b) 1 ps, (c) 10 ps, (d) 35 ps, (e) 220 ps and (f) 7 ns.

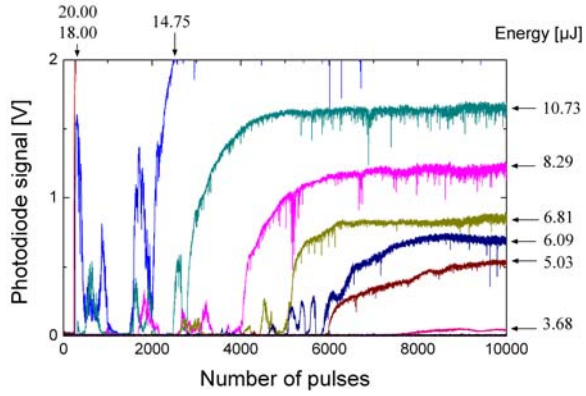

Figure 6: Close-up of figure 5(d) showing spikes in the early stages of drilling.

Another interesting feature is found in figure 5(c), (d) and (e). Early in the drilling process, a "spike" is sometimes observed in which the photodiode signal increases, then decreases with further irradiation (see figure 6). This may occur multiple times before the signal rises permanently for the rest of the drilling. This behavior suggests that the laser beam drilled through the whole sheet followed by the closure of the hole. We attribute the closure of the hole to the deposition of material into the hole. This rise and drop in photodiode signal occurred at approximately the same number of pulses in multiple trials. To confirm that the spikes are not an artefact, additional tests were performed in which the drilling was stopped within the spike. A transmission light microscope was then used to confirm the complete drilling through the sheet.

Finally, from the curves presented in figure 5, the number of pulses to go through the 100 μm thick sheet can be extracted and is plotted in figure 7 as a function of pulse length for various laser energies. The number of pulses to go through the sheet is defined as the point at which an increase in the photodiode signal leads to a permanent opening of the hole (the spikes described earlier are not taken into account here). One can see in figure 7 that the number of pulses required to go through the sheet generally increases with increasing pulse length. As the

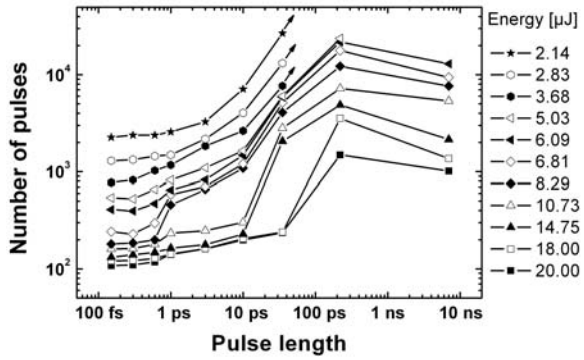

Figure 7: Number of pulses needed to go through a 100μm thick copper sheet as a function of the pulse length for different pulse energies in air.

pulse duration is increased, a sharp increase in the number of pulses is observed for high energies. This increase occurs at longer pulse lengths for higher energies. This could be explained by material redeposition in the hole and could be related to the spike formation. In the 220 ps case, the number of pulses to go through the sheet is relatively high for all energies and for this pulse length, spikes are observed for almost all energies. In the 35 ps case, the two highest energies require relatively few pulses to go through whereas the remaining energies need many more pulses. Interestingly, the two highest energies do not have spikes but the following energies do. In the 10 ps case, the four highest energies require relatively few pulses to go through and spikes start to form only at the fifth highest energy. At 7 ns, the number of pulses to go through is relatively low again and no spikes are observed on the photodiode signal. This suggests that after a spike formed, many more pulses are then required to drill through the hole. These results suggest the importance of material redeposition and hole closure on the drilling efficiency.

4.3 Hole morphology

The wall morphology of the holes has been investigated by cross sectioning the holes along their length using a microtome. Figure 8 shows selected SEM micrographs from near the middle of hole cross sections for samples machined in air with an energy of 10 μJ, 30000 pulses and pulse lengths of 150 fs, 1 ps, 10 ps, 35 ps, 220 ps and 7 ns. For pulse lengths between 150 fs and 1 ps (including 300 fs and 600 fs), regular ripples are seen on the wall of the holes. However, for a pulse length of 10 ps and 35 ps, in addition to areas of ripples, smoother sections are present, suggesting that large quantities of material were molten. The ripple spacing does not significantly change with pulse length and is around 300 nm. A previous investigation has suggested that these ripples are the result of light interference effects [22]. For pulse lengths of 220 ps and 7 ns, only smooth material is seen indicating substantial melting and resolidification. When the holes are drilled in vacuum (figure 9), the rippled structure does not form but instead the surface appears as if liquid droplets impinged on the surface and resolidified rapidly. The size of these features is relatively constant up to 10 ps and is about 200 nm. However when increasing the pulse length beyond 10 ps, the size increases significantly (from 350 nm for 35 ps to more than 3 μm for 7 ns). This suggests again that for pulse lengths larger than $\sim$10 ps, longer pulses produce more molten material.

Similar conclusions can be drawn when examining SEM images of the entrance of laser holes drilled using various pulse lengths in air (figure 10). For pulse lengths between 150 fs and 1 ps, fine debris is redeposited on the sample surface. A magnified view of such debris (figure 11) shows its nanoscale structure which mainly consists of vaporized material containing nanoparticles. The amount of vaporized debris decreases in the 10 ps and 35 ps cases and minimal debris can be seen in the 220 ps and 7 ns cases. However, in the latter cases, a tall rim of molten material is forming around the hole and above the sample surface. This again suggests that a transition takes place after few picoseconds between an ablation regime where the material is mainly vaporized to one where it is mainly melted.

5 Atmosphere

Figure 12 shows two holes drilled with a pulse length of 150 fs, a pulse energy of 0.89 μJ and 1000 pulses per hole. One was drilled in air (figure 12(a)) and the other in a vacuum of $\sim$0.1 mbar (figure 12(b)). It is clearly seen that when air is present, material is redeposited on the sample surface but when the hole is drilled in vacuum, the sample

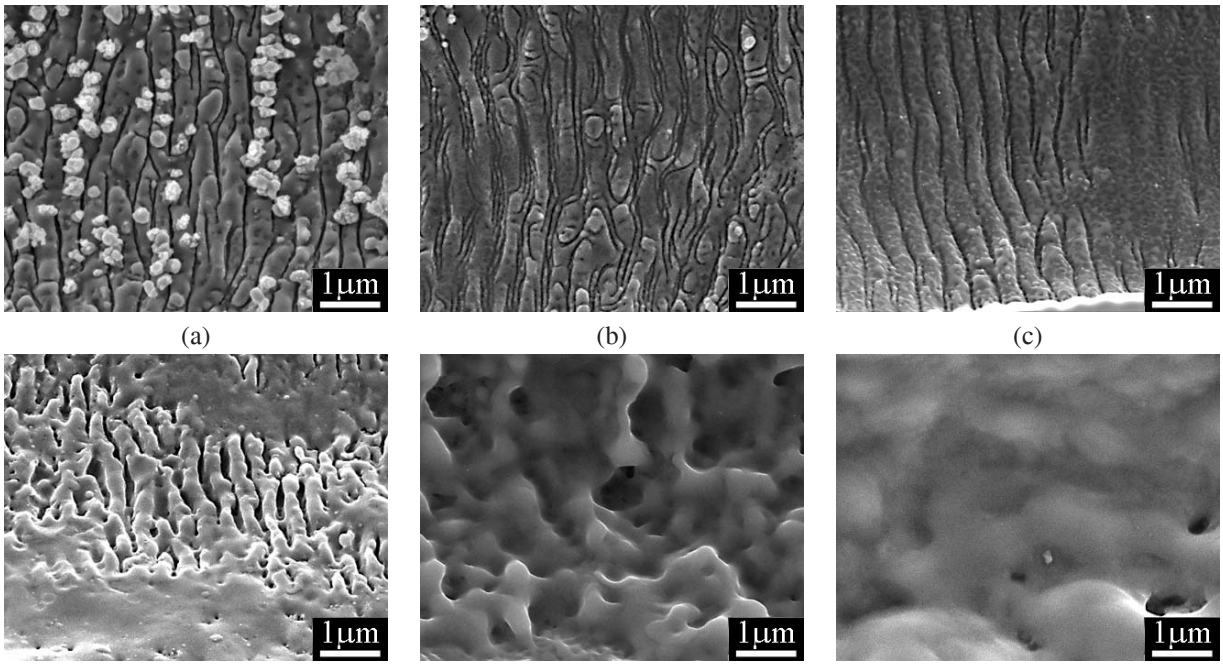

Figure 8: SEM images taken from the middle of laser-produced holes drilled in air using a rotating laser polarization, an energy of 10 μJ and 30000 pulses per hole. The pulse lengths presented here are (a) 150 fs, (b) 1 ps, (c) 10 ps, (d) 35 ps, (e) 220 ps and (f) 7 ns.

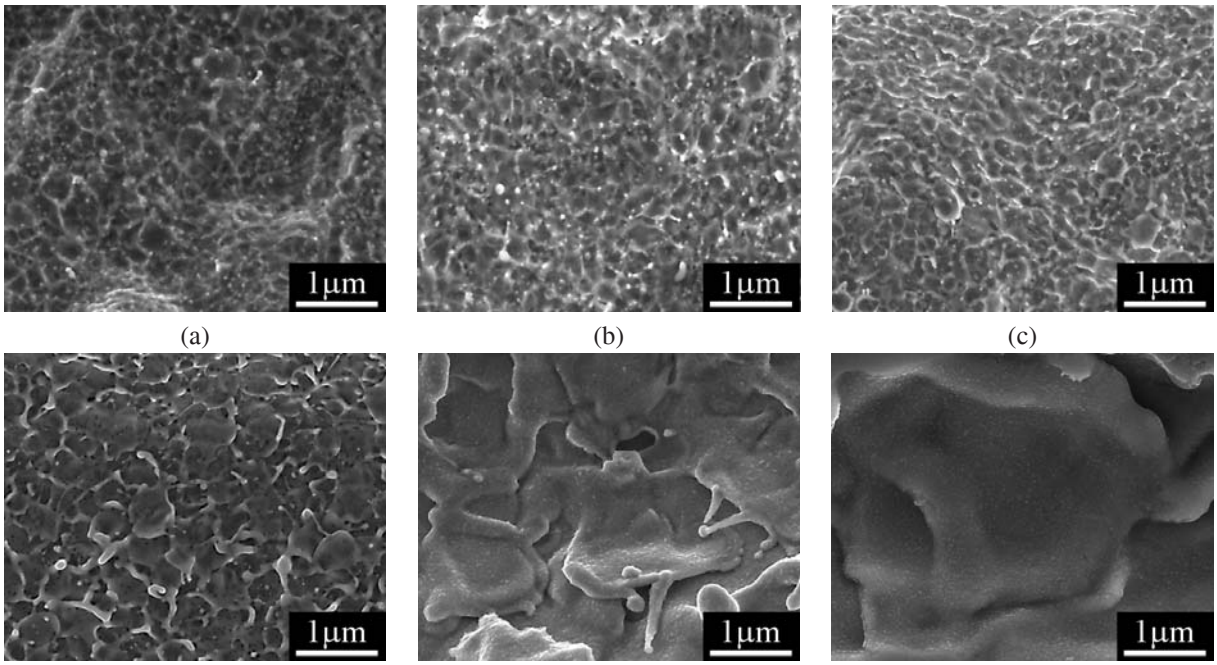

Figure 9: SEM images taken from the middle of laser-produced holes drilled in vacuum using a rotating laser polarization, an energy of 10 μJ and 30000 pulses per hole. The pulse lengths presented here are (a) 150 fs, (b) 1 ps, (c) 10 ps, (d) 35 ps, (e) 220 ps and (f) 7 ns.

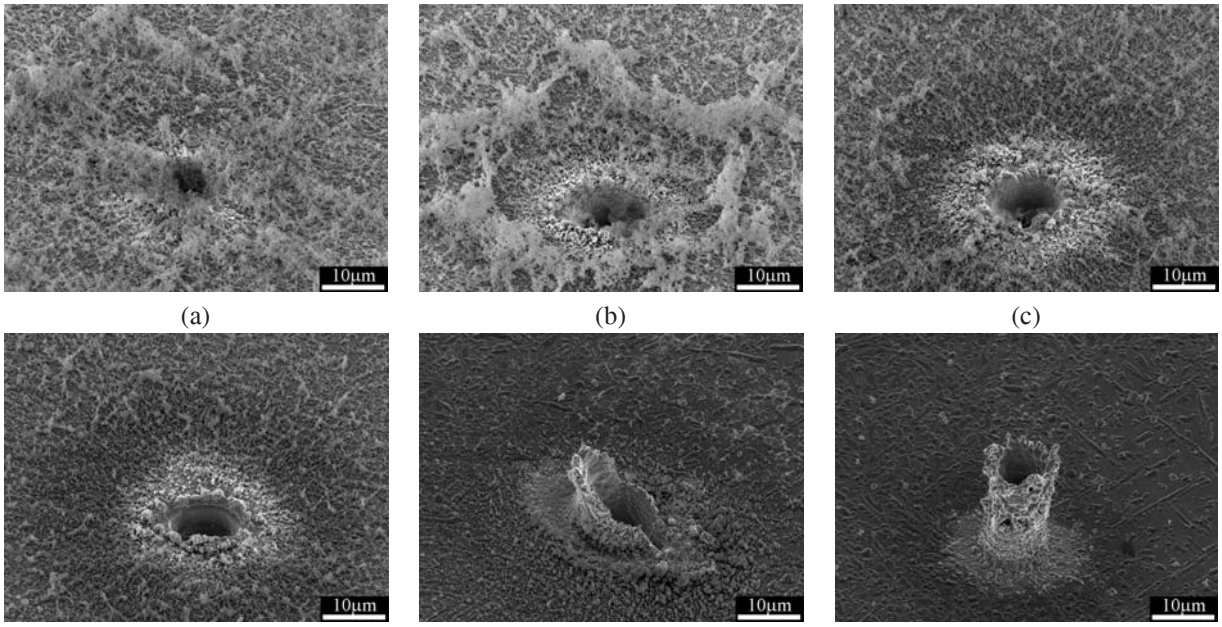

(a) (b) (c)

(d) (e) (f)

Figure 10: SEM images taken from the entrance of laser holes drilled in air using a rotating polarization, an energy of 6.8 μJ and 30000 pulses per hole. The pulse lengths presented here are (a) 150 fs, (b) 1 ps, (c) 10 ps, (d) 35 ps, (e) 220 ps and (f) 7 ns.

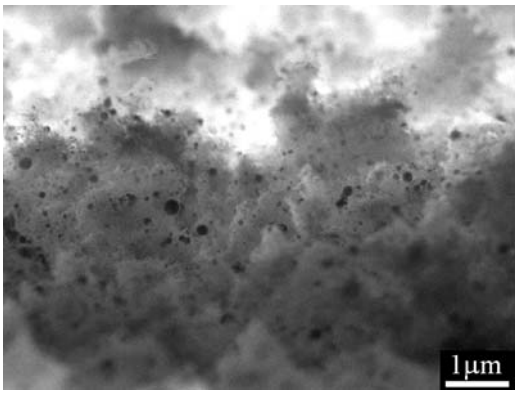

Figure 11: SEM image of the debris deposited close to a 10 ps laser hole drilled in air showing the small copper particles trapped in a much finer nanostructured foam.

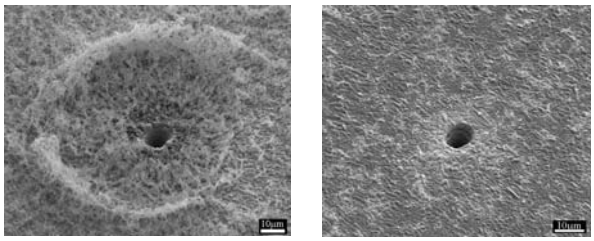

(a) (b)

Figure 12: SEM micrograph of the entrance of a laser hole drilled with a pulse length of 150 fs, an energy of 0.89 μJ and 1000 pulses (a) in air and (b) in vacuum.

surface is much cleaner. A difference between drilling in air versus vacuum is also seen by comparing the photodiode results shown in figure 13 to those in figure 5(c). One can see that for holes drilled in air, the photodiode results are much noisier than when the holes are drilled in vacuum. Furthermore, the number of pulses to drill through a copper sheet (figure 14) shows variations in drilling efficiency when drilling in air or vacuum environments. The results show that drilling in air leads to higher ablation rates at low energies. However, for high energies, the ablation rate is higher in vacuum. We observed this behavior for the two pulse lengths investigated (150 fs and 10 ps). These results are consistent with those of Wynne and Stuart [13] for holes drilled in aluminum and stainless steel.

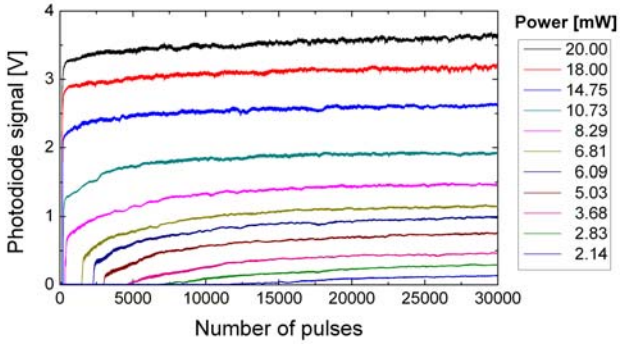

Figure 13: Signal from the photodiode while drilling in vacuum with 10 ps pulses.

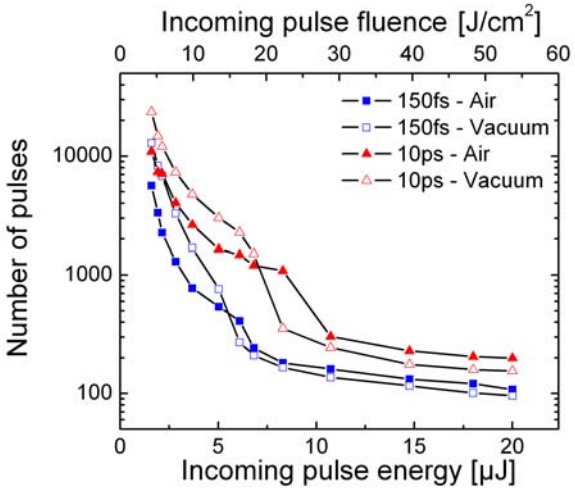

Figure 14: Number of pulses to go through a 100 μm thick copper sheet as a function of laser pulse energy for two pulse lengths in air and vacuum.

6 Summary and conclusions

It has been shown that the number of pulses to drill through a metallic sheet can be accurately determined by recording the energy going through the hole on a photodiode placed under the sample. A steady state is defined when the hole is fully formed and corresponds to the number of pulses at which the intensity on the photodiode no longer varies appreciably. It was found that the entrance hole diameter can be predicted using a simple Gaussian approximation and assuming a material removal fluence threshold of 0.39 J/cm^2 for a pulse length of 150 fs. It was also shown that the energy lost in the hole once the hole is fully formed is almost independent of pulse energy and is on the order of 1 μJ.

At a pulse length of several picoseconds (1-10 ps) there appears to be a transition from the material being mainly vaporized to being mainly melted. The morphology of the walls of laser holes drilled in air with 30000 pulses show that below 10 ps, ripples can be seen and that at 10 ps and above, larger quantities of material have been melted. When holes are drilled in vacuum, the typical size of impacted molten droplets on the wall surface is approximately constant below 10 ps and increases above that pulse length. Finally, observations of the entrance surface of laser holes reveal large quantities of vaporized material for pulse length smaller than 10 ps, while less vaporized and more molten material are seen above 10 ps. This transition pulse length of a several picoseconds is similar to the electron-phonon relaxation time which is on the order of a few picoseconds in copper.

It was shown that at pulse length near a few tens of picoseconds, the laser drilling is perturbed, leading to a fluctuating signal on the photodiode. This perturbation of the transmitted laser beam could be due to plasma formation in the hole. Furthermore, the "spikes" on the photodiode signal suggest that material is redeposited in the hole and causes a significant decrease in the drilling efficiency.

We can conclude that pulse lengths of a few picoseconds ($\sim$1-10 ps) are almost as efficient as their femtosecond counterpart and lead to the same morphologies inside the hole. However, short picosecond systems can have several advantages compared to their femtosecond counterpart such as lower complexity and lower cost (see, eg. [23]). Furthermore, increasing the pulse length to a few picoseconds would greatly reduce the intensity and thus x-ray yield [24], reducing possible health hazards without substantially affecting the final material morphology. Therefore, a few picoseconds would be a pulse time scale of choice in the micromachining of metals.

In a more practical point of view, we showed that a variety of microstructural formations can be obtained in and on the surface of laser drilled holes. Smooth surfaces are generally preferred for precision machining and microfluidics whereas rippled structures can find applications in grating fabrication and adhesion of deposited materials.

Acknowledgement

We gratefully acknowledge the support of the Canada Foundation for Innovation (CFI), the Ontario Innovation Trust (OIT) for infrastructure, the Natural Sciences and Engineering Research Council of Canada (NSERC) and the Canadian Institute for Advanced Research (CIAR). We also thank A. Borowiec for his suggestions concerning the experimental set-up.

References

[1] B. N. Chichkov, C. Momma, S. Nolte, F. von Alvensleben, A. Tünnermann, Applied Physics A-Materials Science and Processing, **63**, 109-115, 1996

[2] S. Nolte, C. Momma, H. Jacobs, A. Tünnermann, B. N. Chichkov, B. Wellegehausen, H. Welling, Journal of the Optical Society of America B-Optical Physics, **14**, 2716-2722, 1997

[3] J. Bonse, S. Baudach, J. Krüger, W. Kautek, M. Lenzner, Applied Physics A-Materials Science and Processing, **74**, 19-25, 2002

[4] D. Ashkenasi, M. Lorenz, R. Stoian, A. Rosenfeld, Applied Surface Science, **150**, 101-106, 1999

[5] T. Q. Jia, Z. Z. Xu, X. X. Li, R. X. Li, B. Shuai, F. L. Zhao, Applied Physics Letters, **82**, 4382-4384, 2003

[6] L. Shah, J. Tawney, M. Richardson, K. Richardson, Applied Surface Science, **183**, 151-164, 2001

[7] S. Juodkazis, H. Okuno, N. Kujime, S. Matsuo, H. Misawa, Applied Physics A-Materials Science and Processing, **79**, 1555 - 1559, 2004

[8] H. Varel, D. Ashkenasi, A. Rosenfeld, M. Wähmer, E.E.B. Campbell, Applied Physics A-Materials Science and Processing, **65**, 367-373, 1997

[9] A. Luft, U. Franz, A. Emsermann, J. Kaspar, Applied Physics A-Materials Science and Processing, **63**, 93-101, 1996

[10] S. Bruneau, J. Hermann, G. Dumitru, M. Sentis, E. Axente, Applied Surface Science, **248**, 299-303, 2005

[11] P. Solana, P. Kapadia, J. Dowden, W. S. O. Rodden, S. S. Kudesia, D. P. Hand, J. D. C. Jones, Optics Communications, **191**, 97-112, 2001

[12] N. N. Nedialkov, P. A. Atanasov, Applied Surface Science, **252**, 4411-4415, 2006

[13] A. E. Wynne, B. C. Stuart, Applied Physics A-Materials Science and Processing, **76**, 373-378, 2003

[14] A. Borowiec, H. K. Haugen, Applied Physics A-Materials Science and Processing, **79**, 521-529, 2004

[15] K. Furusawa, K. Takahashi, H. Kumagai, K. Midorikawa, M. Obara, Applied Physics A-Materials Science and Processing, **69 [Suppl]**, S359-S366, 1999

[16] S. E. Kirkwood, A. C. van Popta, Y. Y. Tsui, R. Fedosejevs, Applied Physics A-Materials Science and Processing, **81**, 729-735, 2005

[17] H. E. Elsayed-Ali, T. B. Norris, M. A. Pessot, G. A. Mourou, Physical Review Letters, **58**, 1212-1215, 1987

[18] C. Schäfer, H. M. Urbassek, L. V. Zhigilei, Physical Review B, **66**, 115404, 2002

[19] M.M. Murnane, H.C. Kapteyn, M.D. Rosen, R.W. Falcone, Science, **251**, 531-536, 1991

[20] S. S. Mao, X. L. Mao, R. Greif, R. E. Russo, Applied Physics Letters, **77**, 2464-2466, 2000

[21] S. S. Mao, X. L. Mao, R. Greif, R. E. Russo, Applied Physics Letters, **76**, 31-33, 2000

[22] A. Weck, T.H.R. Crawford, D.S.Wilkinson, H.K. Haugen, J.S. Preston, Applied Physics A, Online first, DOI: 10.1007/s00339-007-4203-6, 2007

[23] J. Kleinbauer, R. Knappe, R. Wallenstein, Applied Physics B-Lasers and Optics, **80**, 315-320, 2005

[24] J. Thøgersen, A. Borowiec, H.K. Haugen, F.E. McNeill, I.M Stronach, Applied Physics A-Materials Science and Processing, **73**, 361-363, 2001